Spin-glass phase transition revealed in transport measurements

Guillaume Forestier, Mathias Solana, Cécile Naud, Andreas Wieck, François Lefloch, Robert Whitney, David Carpentier, Laurent Lévy, Laurent Saminadayar

Spin-glass phase transition revealed in transport measurements

Guillaume Forestier, Mathias Solana, and Cécile Naud
Institut Néel, Centre National de la Recherche Scientifique, B.P. 166, 38042 Grenoble Cedex 09, France

Andreas D. Wieck
Lehrstuhl für Angewandte Festkörperphysik, Ruhr-Universität, Universitätstraße 150, 44780 Bochum, Germany

François Lefloch
Institut Nanosciences et Cryogénie, Commissariat à l'Énergie Atomique, 17 avenue des Martyrs, 38054 Grenoble Cedex 09, France

Robert Whitney
Laboratoire de Physique et Modélisation des Milieux Condensés, B.P. 166, 38042 Grenoble Cedex 09, France

David Carpentier
Laboratoire de Physique, École Normale Supérieure de Lyon, 47 allée d'Italie, 69007 Lyon, France

Laurent P. Lévy and Laurent Saminadayar*
Institut Néel, Centre National de la Recherche Scientifique, B.P. 166, 38042 Grenoble Cedex 09, France
and Université Grenoble-Alpes, B.P. 53, 38041 Grenoble Cedex 09, France

(Received 4 May 2018; revised 5 May 2020; accepted 14 May 2020; published 31 July 2020)

We have measured the resistivity of magnetically doped Ag:Mn mesoscopic wires as a function of temperature and magnetic field. The doping has been made using ion implantation, allowing a distribution of the dopants *in the middle of the sample*. Comparison with an undoped sample, used as a reference sample, shows that the resistivity of the doped sample exhibits nonmonotonic behavior as a function of both magnetic field and temperature, revealing the competition between the Kondo effect and the RKKY interactions between spins. This proves that transport measurements are still a reliable probe of the spin-glass transition in nanoscopic metallic wire doped using implantation.

DOI: 10.1103/PhysRevB.102.024206

Spin glasses are one of the most fascinating states of matter. They have attracted the interest of a large community for several decades, as it is one of the most fundamental problems in condensed matter physics [1]. A spin glass appears when magnetic atoms are randomly diluted in a nonmagnetic metallic host. As the spatial distribution of the spins is random, the Ruderman-Kittel-Kasuya-Yoshida (RKKY) interactions between the spins [2], which depend on the distance between them, are also random: This leads to frustration between the magnetic moments. It is this interplay between disorder and frustration which is at the basis of the formation of a *spin glass* below a transition temperature T_{sg}. It has been shown recently, using a very tricky experiment, that this subtle scenario for the formation of a spin glass is actually the real one [3]. The very nature of the ground state is still heavily debated and may consist of an unconventional state of matter with remarkable behaviors [4]. Let us mention, however, that spin glasses may also appear in insulating systems [5,6]: This peculiar situation will not be discussed in this paper as it is focused on transport measurements. Finally, it is worth mentioning that spin glass models have also been applied to sociology, biology [7], economy [8,9], and games [10] and are deeply connected to mathematics (topology) [11].

The spin-glass transition itself is quite subtle to detect. In contrast with other phase transitions, there is, for example, no divergence of the specific heat at the transition temperature, but rather a cusp in the (low-frequency) magnetic susceptibility [6]. This has been the most commonly used technique to detect the transition down to very low concentrations of magnetic impurities [12]. More surprising is the onset of irreversibility in the glassy phase: magnetization measured during a cooldown under magnetic field [field cooled (FC) procedure] is completely different from the magnetization obtained when the magnetic field is applied *after* cooling the sample [zero field cooled (ZFC) procedure]. This discrepancy between these two measurements appears exactly at the spin-glass transition temperature [13,14]. This onset of irreversibility is one of the most characteristic signatures of the spin-glass transition.

Another way to probe the spin glass state and the spin glass transition consists of measuring transport properties.

*saminadayar@neel.cnrs.fr

Historically, people were interested in measuring Kondo effect as a function of the concentration of magnetic impurities. For high doping levels, they observed deviations from the well known logarithmic Kondo-like increase of the resistivity: Below a certain temperature, the resistivity exhibits a broad maximum followed by a subsequent decrease [15–18]. Such a behavior was interpreted as a transition to a spin-glass state as spin-spin interactions become predominant. This interpretation was supported by theoretical work [19] which relates the maximum in the resistivity at a temperature T_g to the spin-glass transition. Another natural way to detect changes in the spin configuration of a metal consists of measuring the anomalous Hall effect [20,21]. As interactions between spins become predominant, anomalous Hall resistance exhibits a broad maximum followed by a rapid decrease as the number of free (unfrozen) spins becomes smaller and smaller [22]. A more subtle and difficult way to probe the spin-glass phase consists of measuring the resistance noise of a metallic spin-glass sample [23]. Finally, it should be stressed that the most striking feature of the Kondo physics has also been observed in transport measurements: The onset of irreversibility has been observed in field-cooled (FC)/zero-field cooled (ZFC) resistivity measurements [24].

The question of the existence of a spin-glass transition for small systems has been largely addressed theoretically using numerical simulations. Using state-of-the-art computing facilities [25], it has been shown that samples as small as $30 \times 30 \times 30$ spins already exhibit a spin-glass transition [26–28]. Experimentally, the situation is much more complex: In a mesoscopic sample (i.e., containing few spins), magnetic signals become too small to be detected, even using the most sensitive techniques like SQUID measurements. It is thus tempting to use *transport* measurements to detect the spin-glass transition, as resistivity measurement can easily be performed on nanometer-size samples. This technique has been used in the past to measure the temperature dependance of the resistivity of Kondo systems [29]: The idea was to detect the effect of the finite size of the sample on the development of the Kondo cloud and thus on the screening of the magnetic impurities by the conduction electrons.

Metallic spin glasses are usually obtained by dilution of magnetic impurities in the host metal. Below a critical concentration at which an alloy is formed, impurities will end up in interstitial positions and the crystal structure of the host metal is preserved. The main problem of this technique, however, is that impurities may move during the evaporation and form clusters. Determination of the actual concentration and actual spin of the impurities are then sometimes delicate. An alternative technique consists of implanting ions in the metallic host [30]. This technique allows us to control perfectly the dose implanted [31] and to avoid any clustering as energy barriers forbid any displacement of ions at room temperature. Two points, however, differ between these two techniques: During an implantation, the concentration of the ions through the thickness of the sample presents a gaussian distribution. Very few ions are present at the surface and spin glass physics should not be modified by surface effects as it has been sometimes alleged. Moreover, ions are implanted at high energy: Damages are thus induced in the crystalline structure of the host metal. As RKKY interactions

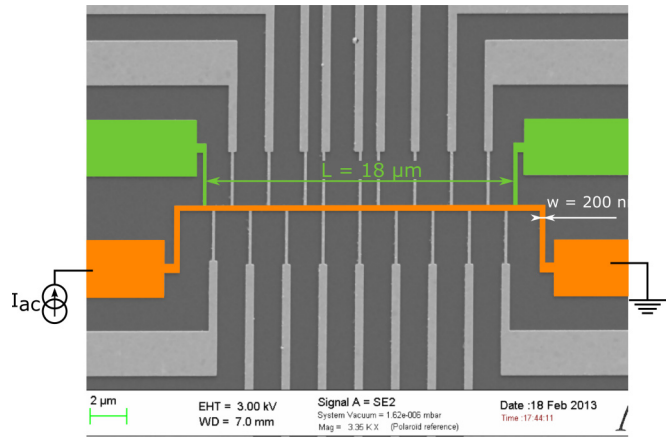

FIG. 1. Electron micrograph of the sample. The wire is 18 μm long, 200 nm wide, and 50 nm thick. Several voltage probes are set along the wire distant by 2 μm.

are mediated by conduction electrons, spin glass transition is a many impurities problem: The equivalence between these two implantation techniques, from a physical point of view, is an interesting and sensible question.

In this paper, we report on transport measurements on nanometer-size mesoscopic Ag:Mn spin glasses at very low doping level. Doping has been obtained by ion implantation technique. Measurements have been performed down to very low temperature (50 mK) and up to high magnetic field (8 T). We show that the behavior of the resistivity can be perfectly explained by an interplay between the Kondo effect and a spin-glass phase transition. This proves that our mesoscopic samples exhibit a phase transition similar to what is observed for macroscopic samples and that the implantation process, although producing crystalline defects, does not change the spin glass physics in such confined geometries. The observed transition temperature is identical to the one detected previously on macroscopic samples doped by standard dilution techniques and with the same doping level using magnetic measurements.

Samples have been fabricated on a silicon/silicon oxide wafer using standard electron-beam lithography on polymethyl-methacrylate resist. Geometry of the sample consists of a long (length $L \approx 18$ μm) and thin (width $w \approx$ 200 nm, thickness t $\approx$ 50 nm) wire (see Fig. 1). Several contacts have been put along the wire, in order to measure the resistance over different lengths and to thermalize properly the electrons along the wire [32]. Silver has been evaporated using a dedicated electron gun evaporator and a 99.9999% purity source with no adhesion layer. Samples have then been implanted with Mn^{2+} ions of energy 70 keV. This energy has been chosen after numerical simulations based on calculations using the SRIM software [31] in order to ensure that ions will end up in the sample following a gaussian distribution whose maximum lies in the middle of the sample thickness. This technique of implantation allows us to avoid clustering or migration of the Mn^{2+} ions as no further annealing has been performed on the samples. The ion dose, measured *via* the current of the implanter, has been chosen in order to give a final ion concentration in the wire of 500 ppm. For this

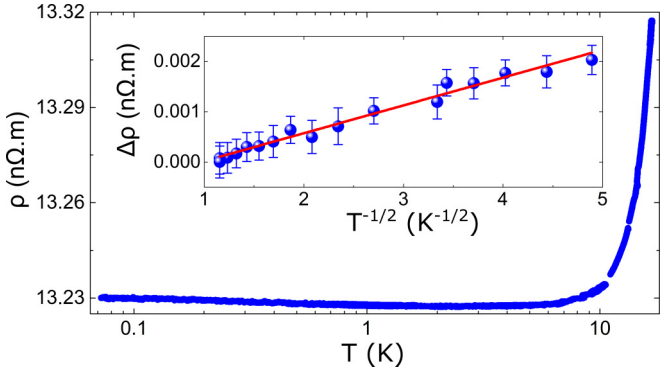

FIG. 2. Resistivity as a function of temperature for the pure Ag sample. Inset: low temperature part ($T \leqslant 1$ K) plotted as a function of $1/\sqrt{T}$. The red line is a fit of the data using Eq. (1).

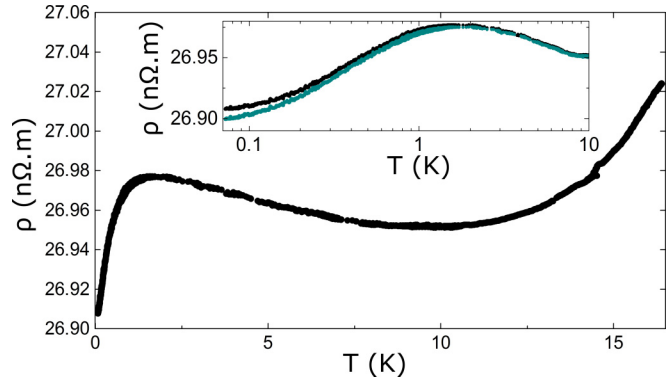

FIG. 3. Resistivity as a function of temperature under zero field of the Ag:Mn spin glass sample doped at 500 ppm. Inset: The black curve is the same data on a logarithmic scale, while the green curve has had the electron-electron interaction contribution subtracted.

concentration of magnetic impurities, the number of spins in a section of the wire is approximately 450. This number is quite small (typically a 15×30 network of spins) and can be reasonably compared with the dimensions of state-of-the-art numerical simulations. Finally, note that some samples have been left unimplanted (pure) in order to be used as reference samples.

Samples have been cooled down in a dilution fridge whose base temperature T is ≈50 mK and equipped with a two-axis superconducting coil of maximum magnetic fields $B_z = 8$ T (out-of-plane field) and $B_{xy} = 1.5$ T (in-plane field). Transport measurements have been carried out using an ac lock-in technique at a frequency of 11 Hz in a bridge configuration and a very low ac current in order to avoid any overheating of the sample. In particular, we have kept $eV_{\rm ds} \leqslant k_B T$ with $V_{\rm ds}$ the drain-source voltage, e the charge of the electron, and k_B the Boltzmann constant. We have seen no dependance of the resistivity on the frequency of the excitation up to our experimentally accessible possibility (≈100 kHz). The signal is amplified using an ultra-low noise homemade voltage amplifier (voltage noise $S_v = 500\ \mathrm{pV}/\sqrt{\mathrm{Hz}}$) at room temperature. All the measuring lines connecting the sample to the experimental setup consist of lossy coaxes which ensure a very efficient radio-frequency filtering and thus a good thermalization of the electrons in the sample [33–35]. At 4.2 K, the resistance of our samples is $R \approx 10\ \Omega$ for the pure samples and $R \approx 30\ \Omega$ for the doped ones.

The resistivity of the pure sample as a function of temperature is depicted in Fig. 2 (a small magnetic field of ≈1000 G is applied in order to cancel the weak localization correction [36]). At high temperature, the resistivity is dominated by electron-phonon interaction and thus decreases rapidly with decreasing temperature. At low temperature, one observes a slight increase of the resistivity; this is typical of mesoscopic samples, in which electron-electron interactions modify the density of states at the Fermi energy [36]. The resistance R of the sample as a function of the temperature T is then given by:

$$R(T) = 0.782\lambda_\sigma \frac{R^2}{R_K}\frac{L_T}{L} = \frac{\alpha}{\sqrt{T}}, \qquad (1)$$

where $L_T = \sqrt{\hbar D/k_B T}$ is the thermal length, D the diffusion coefficient, $R_k = h/e^2$ the quantum of resistance with h the Planck constant and e the charge of the electron, and λ_σ a constant related to the screening parameter of the Fermi liquid theory [36]. For silver, $\lambda_\sigma \approx 3.1$. The inset of Fig. 2 shows the resistance of the pure sample as a function of $1/\sqrt{T}$. As expected, we observe a nice linear behavior down to 50 mK, proving that the electrons are indeed cooled down to the lowest temperature [37].

The same measurements on the doped wire are depicted in Fig. 3. The behavior is clearly different: At low temperature, one observes a pronounced minimum, followed by an increase of the resistivity and an abrupt decrease at very low temperature. The temperature dependence of the resistivity can be separated into four terms:

$$\delta\rho(T) = \delta\rho_{\text{e-ph}}(T) + \delta\rho_{\text{e-e}}(T) + \delta\rho_{\text{e-mag}}(T) + \delta\rho_{wl}(T) \quad (2)$$

corresponding, respectively, to the electron-phonon interaction, electron-electron interaction, and electron-magnetic impurity contribution to the resistivity (which is absent for the pure sample). The term $\delta\rho_{wl}(T)$ corresponds to the quantum correction to the conductivity (weak localization).

This magnetic contribution arises from two distinct phenomena. The first one is the well-known Kondo effect while the second corresponds to the formation of a spin-glass state. It has to be noted that those two effects do not emerge from the same processes. The Kondo effect is due to the scattering of conduction electrons off up-down degenerated magnetic impurities *in the single impurity limit*. The typical energy for this process is the Kondo temperature T_K. Such a behavior has been extensively studied and leads to a logarithmic temperature dependence of the resistivity [38] as the temperature is reduced.

In order to fit the data, we use Hamann's law [39] which is a high ($T \gg T_K$) temperature expansion for the resistivity in the Kondo regime:

$$\rho_{\text{Kondo}}(T) = \frac{\rho^0_{\text{Kondo}}}{2}\left(1 - \frac{\ln(T/T_K)}{\sqrt{\ln^2(T/T_K) + \pi^2 S(S+1)}}\right) \quad (3)$$

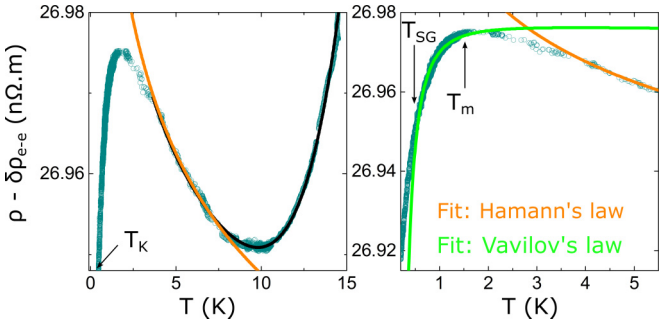

FIG. 4. Resistivity of the spin-glass sample as a function of temperature and after subtraction of the electron-electron interactions contribution to the resistivity. Left panel: orange line is a fit using Hamann's law [Eq. (3)]. Black line is the same fit but adding a power law to take into account the phonon scattering at "high" T. Right panel: same data but restricted to the 0.05–5.5 K temperature range. Green line is a fit using Vavilov's equation [Eq. (5)] which describes the emergence of the spin-glass phase and the corresponding decrease of the resistivity. The different arrows indicate T_K as the Kondo temperature, T_{sg} as the spin-glass transition temperature, and T_m as the temperature of the maximum in the $\rho(T)$.

with S the spin of the magnetic impurities and ρ^0_{Kondo} a constant given by:

$$\rho^0_{\text{Kondo}} = \frac{4\pi\hbar c_{\text{imp}}}{ne^2 k_F} \tag{4}$$

with n the electronic density, c_{imp} the concentration of magnetic impurities, e the charge of the electron, and k_F the Fermi wave vector. Resistivity of the sample as a function of temperature is depicted in the left panel of Fig. 4. The orange line is a fit for $T > 4$ K using equation (3), with the fitting giving $S = 5/2$ and $T_K = 40$ mK. These values are in good agreement with those found in the literature [40] for diluted manganese ions in silver.

At "high" temperature (from 4 K to 15 K) the main contribution to the resistivity is due to the electron-phonon scattering. To take into account for this scattering, we have added to Hamann's law a power law αT^n. Remarkably, this combination of Kondo effect and electron-phonon scattering describes the experimental data very well between 4 K and 15 K.

At "low" temperature (below 4 K), the resistivity deviates from this simple Kondo description as the spin-glass behavior starts to be prominent. Indeed, at those temperatures, RKKY interactions between magnetic impurities are no more negligible, leading to a progressive lift of the up-down spin degeneracy. The density of spins c_{imp} involved in the Kondo processes is thus lowered, leading to a decrease of the resistivity. In this regime, the diffusion mechanisms are completely different and much more complex to calculate. This is related to the appearance of the spin-glass state which is fundamentally very complicated to apprehend. Recent theoretical works have been able, however, to obtain an analytical expression for $\rho(T)$ by simplifying the RKKY interactions to interactions within impurity pairs [41,42]. In the limit where $T_{sg} \gg T_K$, as in our case, this leads to:

$$\rho(T) = \frac{A}{\ln^2(T/T_K)}\left(1 - \alpha_S \frac{T_{sg}}{T}\right), \tag{5}$$

where A is a constant and α_S a constant which depends on the spin S (for $S = 5/2$, $\alpha_S = 2.33$). The temperature of the maximum in the $\rho(T)$ curve, corresponding to the transition between the high temperature phase and the spin-glass one, is then given by:

$$T_m \simeq \frac{\alpha_S}{2} T_{sg} \ln \frac{T_{sg}}{T_K}. \tag{6}$$

In the right panel of Fig. 4, we have plotted the low temperature part of the resistivity of the spin-glass sample. The green line is a fit using equation (5) with $T_K = 40$ mK. The fit is in rather good agreement, keeping in mind that equation (5) is valid only in the proximity of T_{sg}. From this we obtain that two parameters are $A = 0.124$ and $T_{sg} = 500$ mK. This value of T_{sg} is in perfect agreement with those obtained using magnetization measurements on macroscopic samples at the same doping level [12] (see especially Fig. 3 in this reference). This suggests that even for such small systems, a spin-glass transition appears at the same temperature as for macroscopic systems. It must be stressed, however, that only a complete study including measurements of thermodynamic quantities (specific heat, magnetization) could unambiguously lead to this conclusion. Such measurements are, unfortunately, very difficult on such small samples. The two arrows on the right panel of the Fig. 4 indicate the spin-glass transition temperature T_{sg} (left arrow) and the temperature corresponding to the maximum of the $\rho(T)$ curve T_m (right arrow). Using equation (6) with the parameters determined above, we obtain the theoretical temperature of the maximum $T_m \approx 1.5$ K, which is precisely what is observed experimentally. Considering Fig. 4, one can see that these resistivity measurements can be very well described considering the system as a metallic spin glass at low temperature and as a Kondo system at high temperature. It should be noticed than between 2.5 and 3.5 K, experimental data deviate from both fits. This region corresponds to the range of temperature where Kondo effect and RKKY interactions compete with almost equal strength and no theoretical approach is able to completely describe this mixed behavior.

Finally, in order to characterize the effect of the magnetic field on the resistivity of the sample, we have performed high field magnetoresistance measurements at different temperatures. For this purpose, we use the zero field cooled (ZFC) protocol: The sample is cooled down under zero field and the magnetic field is applied at low temperature. The relative variation of the resistivity, $\Delta\rho/\rho_0 = (\rho(B) - \rho(B = 0))/\rho(B = 0)$, has been plotted in Fig. 5 for temperatures down to 200 mK (i.e., $T \ll T_{sg}$) and up to 20 K (i.e., $T \gg T_{sg}$). At high temperature ($T \gg 10$ K), curves are perfectly superimposed and the magnetoresistivity is perfectly quadratic in B, as can be seen in Fig. 6. In this regime, the resistivity is dominated by electron-phonon scattering, and one recovers the classical quadratic magnetoresistance of metals. In order to extract the magnetic contribution to the magnetoresistivity, we have subtracted the high temperature contribution in Fig. 6 from the data in Fig. 5. The result, plotted as a function of

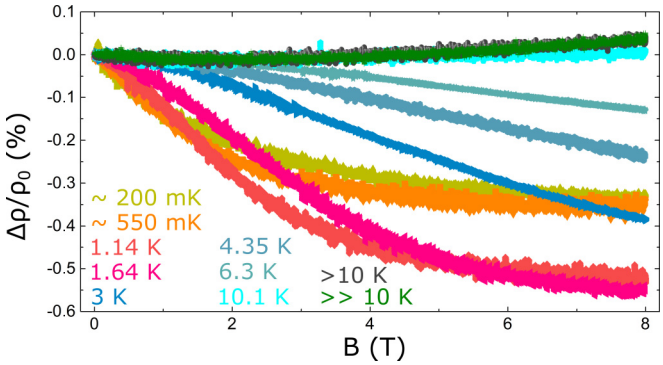

FIG. 5. Relative magnetoresistivity of a 500 ppm spin glass sample for different temperatures.

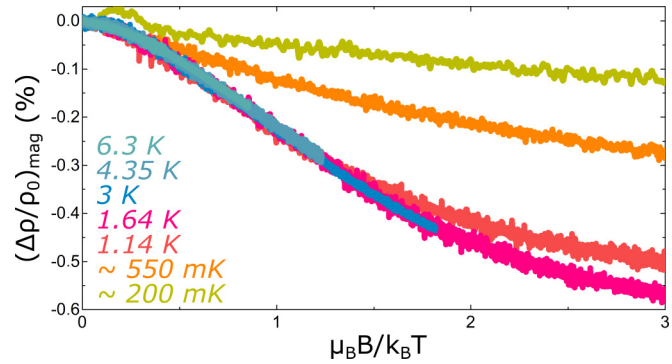

FIG. 7. Relative magnetoresistivity of a 500 ppm spin glass sample as a function of the normalized magnetic field for different temperatures. The classical B^2 contribution has been subtracted.

the normalized magnetic field $\mu_B B/k_B T$, with μ_B the Bohr magneton, is depicted in Fig. 7.

For temperatures larger than 1.5 K, all the curves are rather well superimposed. This means that, in this range of temperature, the resistivity depends only on the ratio $\mu_B B/k_B T$, which is proportional to the polarization, i.e., the number of free spins [19,43] (Curie's law). As mentioned above such behavior is typical of the Kondo effect as it is a single impurity process.

Below 1 K, however, we observe strong deviations to this behavior, showing that Kondo physics is not the good description anymore. Note that this is the temperature at which the $\rho(T)$ exhibits a maximum (see Fig. 4). It is quite surprising that deviations from Kondo physics appear at such high temperature as compared to the spin glass transition temperature. We would like to stress, however, that recent measurements of universal conductance fluctuations on mesoscopic spin glass wires suggests that spin-spin interactions already play a role well above T_{sg} [30]. Whether this is due to the nature of the transition itself or to the reduce dimensionality of these mesoscopic samples is still an open and intriguing question.

Similar behavior can be observed on the temperature dependance of the resistivity under magnetic field. This measurement is depicted in Fig. 8. As we have seen previously, under zero field, the competition between Kondo physics and spin-spin interactions leads to a broad maximum in the $\rho(T)$ curve. Under magnetic field, the maximum observed in the $\rho(T)$ curve is progressively suppressed and shifted towards higher temperatures. This is due to the fact that the field progressively suppresses the up-down degeneracy and thus the Kondo effect. The slope of the logarithmic increase in $\rho(T)$ becomes weaker: The maximum amplitude in the resistivity thus decreases [43]. Moreover, the shift of the $\rho(T)$ maximum is explained by the fact that, since Kondo effect is reduced, spin-spin interactions become dominant at higher temperatures; note that this still applies *even when magnetic field becomes larger than the typical spin-spin interaction energy* $\mu_B B \gg k_B T_{sg}$.

As a final point, we would like to stress that such a characterization of nanoscopic spin glass wires fits naturally into recent works on mesoscopic spin glasses. In this domain, the goal is to probe magnetic configuration of the spins *via* the dephasing induced on the coherent conduction electrons [36]. The most striking result, reproduced in several experiments [30,44–47], of this exploration of mesoscopic systems is that the configuration of spin glasses are unexpectedly robust against the application of high magnetic fields B ($\mu_B B \gg k_B T_{sg}$): Upon cycling samples under magnetic field of several Tesla, universal conductance fluctuations are *perfectly reproducible*, meaning that the spins are in the exact same configuration before and after the application of the field. Our work,

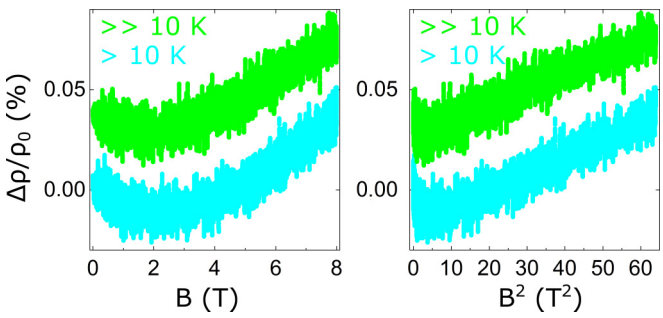

FIG. 6. Relative magnetoresistivity of a 500 ppm spin glass sample for temperatures larger than 10 K plotted as a function of B (left panel) and B^2 (right panel) (same data as Fig. 5). Blue curve represents data measured at 10.1 K when the relative magnetoresistance starts to be positive (see Fig. 5). Green curve represents data measured well above 10, i.e., far in the saturated regime (it has been shifted for a sake of clarity).

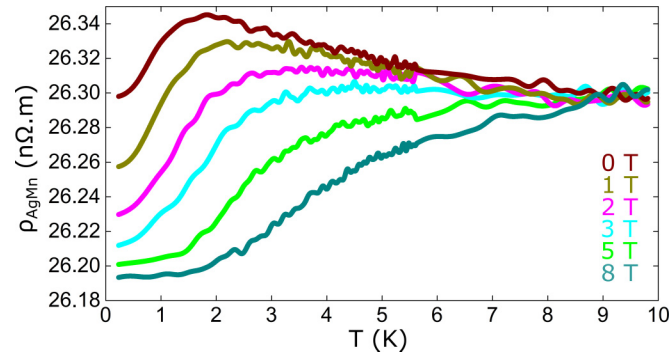

FIG. 8. Resistivity of a 500 ppm spin glass sample as a function of temperature under different magnetic fields.

if it does not shed new light on this strange and remarkable experimental fact, gives some hints for its interpretation as it excludes the hypothesis that it may be due to an absence of spin glass transition in nanoscopic samples.

As a conclusion, we have measured the magnetoresistivity of a 500 ppm Ag:Mn mesoscopic spin glass wire as a function of temperature and magnetic field. We have explored temperatures ranging from 50 mK ($T \simeq T_K \ll T_{sg}$) up to 10 K ($T \gg T_{sg} \gg T_K$) and magnetic fields up to 8 T ($\mu_B B \gg k_B T_{sg} \gg k_B T_K$). Despite the small number of spins in the section of the wire (typically 15×30 spins), we observe a signature of the spin glass phase transition revealed by a maximum in the $\rho(T)$ curve. Around this maximum, data can be fitted using Vavilov-Glazman's law for the low temperature (spin-glass) part of the curve and Hamann's law for the high temperature (Kondo) part. Moreover, the T_{sg} and T_K extracted from these fits are in agreement with those obtained by magnetic measurements on macroscopic samples. These results are validated by magnetoresistance measurements in which both the dominance of Kondo physics and spin-glass behavior are observed in different range of temperature. This, combined with the recent observation of irreversibility in the resistivity of mesoscopic samples and numerical simulations, proves that, even in such small samples, a spin glass phase transition appears when the temperature is lower than the typical strength of the spin-spin interaction.

We are indebted to H. Pothier and H. Bouchiat for the use of their Joule evaporators. We thank T. Costi, L. Glazman, E. Orignac, H. Bouchiat, É. Vincent, A. Rosch, and H. Alloul for fruitful discussions.

[1] *Les Houches summer school*, Session LXXXV, edited by J.-P. Bouchaud, M. Mézard, and J. Dalibard (Elsevier, Amsterdam, 2006).
[2] C. Kittel, *Introduction to Solid State Physics* (John Wiley & Sons, New York, 2005).
[3] M. Ali, P. Adie, C. H. Marrows, D. GreigBryan, and J. Hickey, Nat. Mater. **6**, 70 (2007).
[4] É. Vincent, J. Hammann, and M. Ocio, J. Stat. Phys. **135**, 1105 (2009).
[5] K. H. Fisher and J. A. Hertz, in *Spin Glasses: An Experimental Introduction* (Taylor & Francis Ltd, London, 1993).
[6] J. A. Mydosh, in *Spin Glasses* (Cambridge University Press, Cambridge, 1991).
[7] K. B. Storey and J. M. Storey, Sci. Am. **263**, 62 (1990).
[8] D. Sornette, A. Johansen, and J. P. Bouchaud, J. Phys. I Fr. **6**, 167 (1996).
[9] U. Krey, arXiv:0812.3378.
[10] A. K. Hartmann, arXiv:1312.1839. See http://www.compphys.uni-oldenburg.de/en//61304.html.
[11] R. Rammal, G. Toulouse, and M. A. Virasoro, Rev. Mod. Phys. **58**, 765 (1986).
[12] G. Frossati, J. L. Tholence, D. Thoulouze, and R. Tournier, Physica B&C **84**, 33 (1976).
[13] D. Sherrington and B. W. Southern, J. Phys. F: Met. Phys. **5**, L49 (1975).
[14] S. Nagata, P. H. Keesom, and H. R. Harrison, Phys. Rev. B **19**, 1633 (1979).
[15] O. Laborde and P. Radhakrishna, J. Phys. F: Met. Phys. **3**, 1731 (1973).
[16] O. Laborde, B. Loegel, and Radhakrishna, J. Phys. Colloques **35**, C4-247 (1974).
[17] P. J. Ford and J. A. Mydosh, Phys. Rev. B **14**, 2057 (1976).
[18] U. Larsen, Phys. Rev. B **14**, 4356 (1976).
[19] M.-T. Béal-Monod and R. A. Weiner, Phys. Rev. **170**, 552 (1968).
[20] H. Vloeberghs, J. Vranken, V. Vanhaesendonck, and Y. Bruynseraede, Europhys. Lett. **12**, 557 (1990).
[21] N. Nagaosa, J. Sinova, S. Onoda, A. H. MacDonald, and N. P. Ong, Rev. Mod. Phys. **82**, 1539 (2010).
[22] T. Taniguchi, K. Yamanaka, H. Sumioka, T. Yamazaki, Y. Tabata, and S. Kawarazaki, Phys. Rev. Lett. **93**, 246605 (2004).
[23] M. B. Weissman, Rev. Mod. Phys. **65**, 829 (1993).
[24] T. Capron, A. Perrat-Mabilon, C. Peaucelle, T. Meunier, D. Carpentier, L. P. Lévy, C. Baüerle, and L. Saminadayar, Europhys. Lett. **93**, 27001 (2011).
[25] L. R. Walker and R. E. Walstedt, Phys. Rev. B **22**, 3816 (1980).
[26] K. Binder and A. P. Young, Rev. Mod. Phys. **58**, 801 (1986).
[27] G. Parisi, Physica A **386**, 611 (2007).
[28] R. Alvarez Baños, A. Cruz, L. A. Fernandez, J. M. Gil-Narvion, A. Gordillo-Guerrero, M. Guidetti, A. Maiorano, F. Mantovani, E. Marinari, V. Martin-Mayor, J. Monforte-Garcia, A. Muñoz Sudupe, D. Navarro, G. Parisi, S. Perez-Gaviro, J. J. Ruiz-Lorenzo, S. F. Schifano, B. Seoane, A. Tarancon, R. Tripiccione, and D. Yllanes (JANUS collaboration), J. Stat. Mech. (2010) P06026.
[29] G. Neuttiens, J. Eom, C. Strunk, V. Chandrasekhar, C. Van Haesendonck, and Y. Bruynseraede, Europhys. Lett. **34**, 617 (1996).
[30] T. Capron, G. Forestier, A. Perrat-Mabilon, C. Peaucelle, T. Meunier, C. Baüerle, L. P. Lévy, D. Carpentier, and L. Saminadayar, Phys. Rev. Lett. **111**, 187203 (2013).
[31] J. F. Ziegler and J. P. Biersack, http://www.srim.org/.
[32] B. Huard, H. Pothier, D. Estèeve, and K. E. Nagaev, Phys. Rev. B **76**, 165426 (2007).
[33] A. B. Zorin, Rev. Sci. Instrum. **66**, 4296 (1995).
[34] D. C. Glattli, P. Jacques, A. Kumar, P. Pari, and L. Saminadayar, J. Appl. Phys. **81**, 7350 (1997).
[35] S. Mandal, T. Baütze, R. Blinder, T. Meunier, L. Saminadayar, and C. Baüerle, Rev. Sci. Instrum. **82**, 024704 (2011).
[36] É. Akkermans and G. Montambaux, *Mesoscopic Physics of Electrons and Photons* (Cambridge University Press, Cambridge, 2007).
[37] F. Mallet, J. Ericsson, D. Mailly, S. Unlübayir, D. Reuter, A. Melnikov, A. D. Wieck, T. Micklitz, A. Rosch, T. A. Costi, L. Saminadayar, and C. Baüerle, Phys. Rev. Lett. **97**, 226804 (2006).
[38] A. C. Hewson, *The Kondo Problem to Heavy Fermions*, Cambridge Studies in Magnetism (Cambridge University Press, Cambridge, 1997).

[39] D. R. Hamann, Phys. Rev. **158**, 570 (1967).
[40] C. Rizzuto, Rep. Prog. Phys. **37**, 147 (1974).
[41] M. G. Vavilov and L. I. Glazman, Phys. Rev. B **67**, 115310 (2003).
[42] M. G. Vavilov and L. I. Glazman, A. I. Larkin, Phys. Rev. B **68**, 075119 (2003).
[43] P. Monod, Phys. Rev. Lett. **19**, 1113 (1967).
[44] F. Schopfer, C. Baüerle, W. Rabaud, and L. Saminadayar, Phys. Rev. Lett. **90**, 056801 (2003).
[45] P. G. N. de Vegvar, L. P. Lévy, and T. A. Fulton, Phys. Rev. Lett. **66**, 2380 (1991).
[46] D. Petit, L. Fruchter, and I. A. Campbell, Phys. Rev. Lett. **88**, 207206 (2002).
[47] M. Solana *et al.* (in preparation).